Pion-Proton Total Cross Sections from 0.45 to 1.9 Bev†

R. Cool, O. Piccioni,* and D. Clark‡
Brookhaven National Laboratory, Upton, New York
(Received April 30, 1956)

Measurements of the pion-proton total cross section over a range of kinetic energies from 0.45 to 1.9 Bev are described. Positive pions were distinguished from protons of the same momentum by a time-of-flight technique. A liquid hydrogen absorber was used for most of the measurements. Muons, the principal beam contamination, were approximately 10% of the pions.

A pronounced maximum for $\sigma(\pi^-,p)$ near 0.9 Bev, which had been noted in our preliminary measurements, is confirmed by data presented here. If this maximum is to be interpreted as a resonance in a single state of angular momentum, the analysis shows that, after subtracting a term which can reasonably be attributed to nonresonant states, the total angular momentum could be as low as 5/2 without serious disagreement with experimental data. The possibility of explaining this maximum with a resonant pion-pion interaction as conjectured by Dyson and Takeda is discussed. The measurements of $\sigma(\pi^+,p)$ also give evidence for the existence of a maximum of relatively smaller amplitude at 1.35 Bev.

The differential cross sections in the forward direction for elastic and charge-exchange scattering of pions by protons have been obtained by making use of the dispersion relations.

I. INTRODUCTION

THE energy dependence of the total cross section for pion-proton collisions below 400 Mev has proved to be a powerful clue to the understanding of meson physics.[1,2] The pronounced maximum in the positive pion total cross section at 195 Mev reaches a value of 200 mb, which for $j=\frac{3}{2}$ is very closely equal to $2\pi\lambda^2(2j+1)$, the maximum value of the cross section for an elastic process occurring in a state of total angular momentum j. This fact, by itself, strongly suggests a resonance-like interaction in a state with total angular momentum $j=\frac{3}{2}$. Moreover, at this energy the ratio of the total cross section $\sigma(\pi^+,p)$ to $\sigma(\pi^-,p)$ is quite close to 3 which is the ratio of the weight of the isotopic spin state $\frac{3}{2}$ in the (π^+,p) system to that of the state $\frac{3}{2}$ in the (π^-,p) system. Thus a second inference naturally follows; the strong interaction, which peaks at 195 Mev, is characteristic of a state with total isotopic spin $T=\frac{3}{2}$. All this constructive evidence obtained with "low-energy" pions made it clear that measurements of the total cross sections of pions with hydrogen should be pursued to higher energies.

Of course, one did not necessarily expect as suggestive information at very high energies as that obtained at low energies, since so many states of angular momentum are present that no one of them is likely to have a preponderant effect on the probability of interaction. In this sense, at the beginning of the experiment, an energy of 1.5 Bev appeared to us to be high, and for this reason, after a first measurement was made at that energy to observe the high-energy trend of the curve, our attention was focused at energies of 1.0 Bev and lower. The cross section near 1.0 Bev for negative pions as measured by Shapiro *et al.*[3] and by us[4] turned out to be larger than at 0.45 Bev[5] and 1.5 Bev.[6] Positive pions did not exhibit any such maximum in the total cross section.

In the process of accumulating data at relatively small energy intervals in order to define the energy dependence of the cross sections, we observed that the $\sigma(\pi^+,p)$ and $\sigma(\pi^-,p)$ curves which cross at about 0.42 Bev, appeared to cross again at an energy of about 1.1 Bev. As a consequence, it was considered opportune to extend a careful study to energies above 1.1 Bev. It was also evident that the differences between the cross sections at different energies, as well as between $\sigma(\pi^+,p)$ and $\sigma(\pi^-,p)$, would be rather small, so that we should measure directly the cross section of positive pions with hydrogen, rather than use the approximate and indirect method of measuring the difference between the negative pion cross section with deuterium and with hydrogen (see Secs. IIA and III for a discussion). Fortunately, at this time we could avail ourselves of the possibility offered by the deflection system developed to obtain an external proton beam.[7] It could be used to make the proton beam strike a target close to the external wall of the vacuum chamber; from that target both positive and negative mesons could be obtained at a small angle with respect to the direction of the primary proton beam.

The first data taken by our group in collaboration with Professor L. Madansky at 1.5 and 1.0 Bev have already been published.[4,6] Subsequently, measurements at these energies have been repeated. Some new data

† Under the auspices of the U. S. Atomic Energy Commission.
* On leave of absence at Radiation Laboratory, University of California, Berkeley, California.
‡ Present address: Cornell University, Ithaca, New York.
[1] K. A. Brueckner, Phys. Rev. **86**, 106 (1952).
[2] For a review of the low-energy results see for example, H. A. Bethe and F. de Hoffmann, *Mesons* (Row, Peterson and Company, White Plains, 1955), Vol. II; M. Gell-Mann and K. Watson in Ann. Revs. Nuclear Sci. **4**, 219 (1954).
[3] Shapiro, Leavitt, and Chen, Phys. Rev. **92**, 1072 (1953).
[4] Cool, Madansky, and Piccioni, Phys. Rev. **93**, 637 (1954); Phys. Rev. **93**, 918(A) (1954).
[5] S. Lindenbaum and L. Yuan, Phys. Rev. **92**, 1578 (1953).
[6] Cool, Madansky, and Piccioni, Phys. Rev. **93**, 249 (1954).
[7] Piccioni, Clark, Cool, Friedlander, and Kassner, Rev. Sci. Instr. **26**, 232 (1955).

have been reported at the Rochester Conference.[8] In this article we report all the data between 0.45 and 1.9 Bev and describe the experimental method in as much detail as may be of use. A careful study made at this laboratory in the energy range from 150 to 700 Mev has already been published by Lindenbaum and Yuan.[9]

II. DESCRIPTION OF EXPERIMENT

A. Pion Beams

The total cross sections have been obtained from "good geometry" attenuation measurements. The beam, as defined by a scintillation counter telescope, impinges on an absorber. Behind the absorber is placed the final counter, larger than those of the telescope, which subtends a cone of semiaperture θ. Those particles which are deviated in the absorber by an angle greater than θ fail to cross the final counter and are counted as having interacted. Since the semiaperture of the cone is not the same at each point of the absorber, owing to its finite length, each geometry is characterized by the average of θ^2 over the length of the absorber, which we call $\langle\theta^2\rangle$. This choice is suggested by considering that $d\sigma/d\Omega$ for the production of secondaries can be assumed to be constant over the angles subtended by the final counter. In this case, the error ϵ in the total cross section, as a result of secondaries which cross the final counter, is approximately

$$\epsilon\cong\pi\langle d\sigma/d\Omega\rangle\langle\theta^2\rangle.$$

In part, the pion-proton cross sections $\sigma(\pi^{\pm},p)$ were obtained from the difference in the attenuation in CH_2 and C, both absorbers containing an equal amount of C. For the remainder, a liquid hydrogen target was used. These measurements gave the same results as the CH_2-C difference whenever both methods were used.

Until recently, positive pions were available only up to about 1.0 Bev. This limitation results from the fact that high-energy pions are produced predominantly at forward angles and are deflected inward by the field of the Cosmotron if they are positive. The consequence is that there is no practical way to place the apparatus in such a beam. On the other hand, negative pions, which are deflected outward, can be readily collimated into a usable beam up to the highest energies.

For high-energy pions whose wavelengths are short compared to the average distance between nucleons in the deuteron and whose elementary cross sections are not too large, the cross section $\sigma(\pi^{\pm},d)$ should be close to the sum $\sigma(\pi^{\pm},p)+\sigma(\pi^{\pm},n)$. Hence, we would expect the cross section $\sigma(\pi^{-}, d-p)$, which is obtained from the attenuation difference of D_2O and H_2O, to be closely equal to $\sigma(\pi^{-},n)$. Moreover, by the well-accepted principle of charge symmetry, $\sigma(\pi^{-},n)=\sigma(\pi^{+},p)$. For this reason, when positive pions were not available, we have

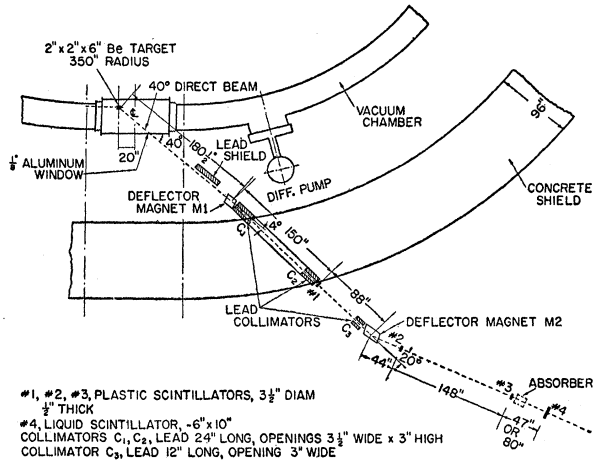

FIG. 1. Schematic arrangement of apparatus, 40° direct beam.

measured $\sigma(\pi^{-}, d-p)$ in order to obtain an approximate value for $\sigma(\pi^{+},p)$.

Either out of necessity in order to cover the range of energies from 0.45 to 1.9 Bev, or in order to be compatible with other experiments being carried on simultaneously, several beams have been used while performing this series of measurements. Targets can be placed in the field-free "straight sections" of the Cosmotron in such a position that pions, produced at angles greater than 32° with respect to the direction of the proton beam, pass out of the Cosmotron with negligible magnetic deflection. We have used two different such "direct beams," one at 40°, the other at 32°. The 40° beam was used between 0.45 and 0.80 Bev; the 32° beam between 0.80 and 1.08 Bev. Above 1.08 Bev the intensity of pions becomes too low for practical measurements in these beams. For lower energies, these direct beams have the advantage that both positive and negative pions are available. By simply adjusting the current in the external magnets and changing its direction, all momenta and both charges of pions could be investlgated without moving the apparatus. Figure 1 shows a typical arrangement of the apparatus.

Negative pions, produced near the forward direction, are deflected outward by the magnetic field of the Cosmotron and pass through collimators in the concrete shield. The Cosmotron magnet thus provides a momentum analysis of the pions and for suitable target positions there is a moderate focusing action in the horizontal plane. Usually, an external magnet is also required in order to sweep out of the beam secondary particles produced in the collimator and in the wall of the vacuum chamber. To optimize the intensity for a given target position and machine energy, the apparatus and collimator must be moved for each new momentum selected. One can, however, make a small change in the selected pion momentum by making a proportional change in the final primary proton beam momentum (i.e., in the final magnetic field of the Cosmotron) with-

[8] Cool, Piccioni, and Clark, *Proceedings of the Fourth Annual Rochester Conference* (University of Rochester Press, Rochester, 1954), p. 101; *Proceedings of the Fifth Annual Conference on High-Energy Physics* (Interscience Press, Inc., New York, 1955), p. 38.

[9] S. Lindenbaum and L. Yuan, Phys. Rev. **100**, 314 (1955).

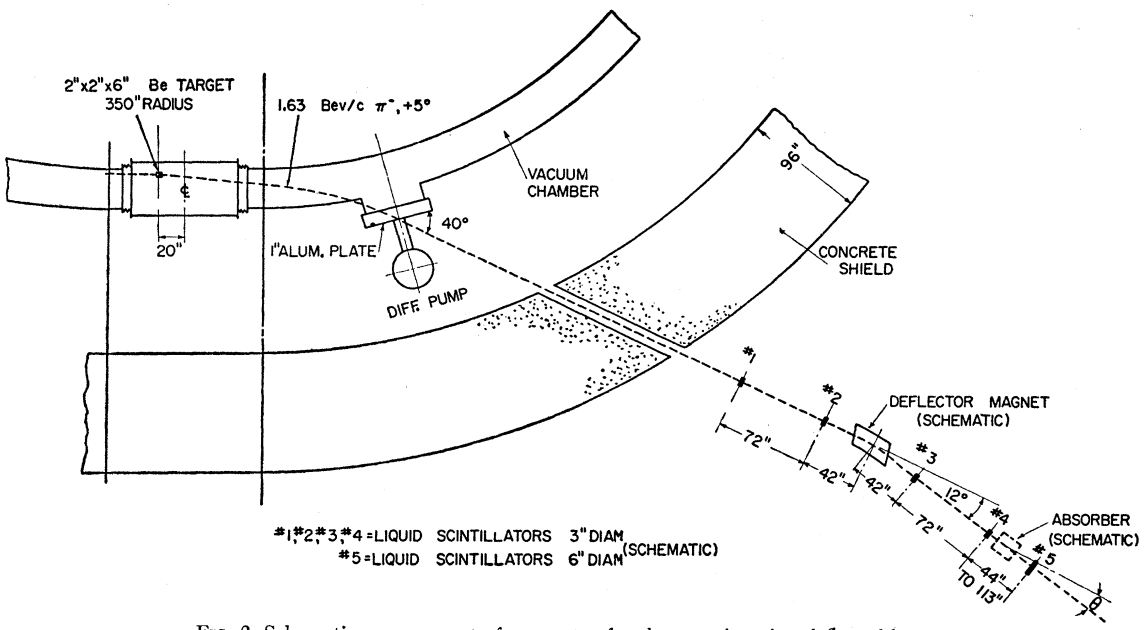

FIG. 2. Schematic arrangement of apparatus for the negative pion deflected beams.

out changing the trajectory as defined by the collimator and counters. This method is useful for only relatively small momentum changes because lowering the primary proton momentum also results in a decrease in pion production; further, the fringing field is not strictly proportional to the orbit field and will change somewhat the direction of the trajectory for the selected momentum. Figure 2 shows schematically the trajectories and apparatus used in the course of experiments in the "deflected beams."

During the last stage of the experiment, the development of an ejection system for the proton beam allowed us to place a target at such a position that pions produced at an angle of 5.5° to the forward direction could leave the Cosmotron without having crossed any appreciable magnetic field. This arrangement is illustrated in Fig. 3. This beam, although we have used it primarily to obtain high-energy pions, can be used universally for positive and negative pions of any desired energy. Clearly, all of our measurements could have been made in this beam.

The circulating proton beam which enters the ejection magnet $M1$ (the ejection system is described in detail elsewhere)[7] is deflected outward and strikes a Cu target

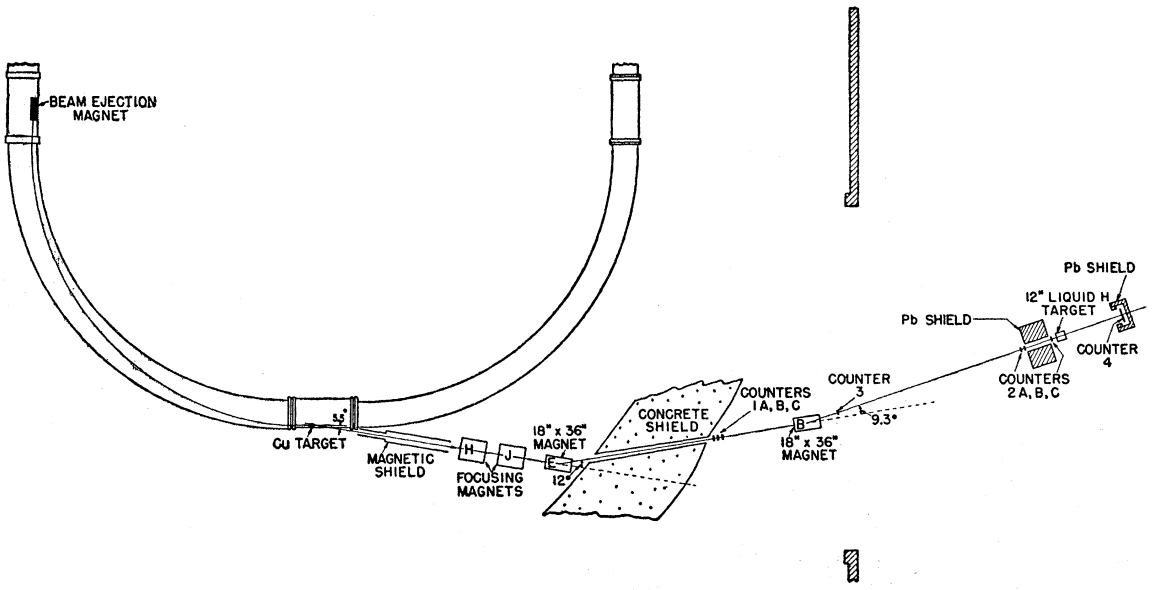

FIG. 3. Schematic arrangement of apparatus in 5.5° direct beam using magnetic focusing.

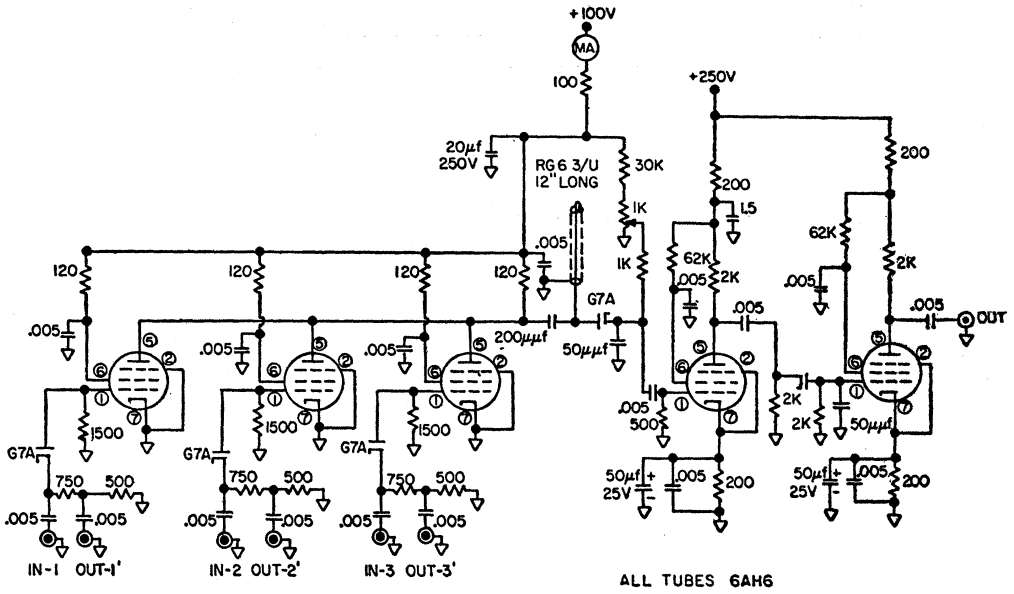

FIG. 4. Fast triple-coincidence circuit using a plate clipping line.

which is placed at the outer edge of the magnetic-field-free "straight section." The efficiency of the ejection system is such that about one-half of the circulating proton beam strikes the target. The circulating beam is also somewhat reduced, perhaps by as much as a factor of 2, by the presence of the magnet inside the evacuated volume of the Cosmotron. Pions, which are produced in a small cone near 5.5° to the forward direction of the protons, pass through a magnetic shield which reduces the fringing field of the Cosmotron to a value less than 50 gauss, so that the deflection of the pions within the magnetic shield is small. The large (12 in.) quadrupole strong-focusing lens (shown as H and J in Fig. 3) focuses an image of the target outside the concrete shield. The position of the image can be varied by adjusting the currents in the magnets. The focusing action of the magnetic lens increases the solid angle of acceptance for the pions and, therefore, increases the intensity of pions per unit momentum interval by perhaps more than a factor of ten. The counting rate in our telescope was about 140 positive pions of 1.0-Bev kinetic energy per 10^{10} circulating 3-Bev protons. For 1.67-Bev kinetic energy, there were 90 positive pions per 10^{10} protons. The momentum spread, as computed, was $\pm 2.0\%$ and the diameter of the counter telescope was 3 inches.

B. Counters

The telescope that defines the beam of pions consisted of plastic scintillators one-half inch thick, either three or three and one-half inches in diameter. Each scintillator was viewed by two RCA 1P21 photomultipliers with their plates simply connected together. A germanium diode G7A was also shunt-connected to the plates to limit the output pulse at approximately 1 volt.

The final counter, which detects the particles that have not interacted, was of a large diameter, so that the cross-sectional area of the beam, with no absorber, was appreciably less than the area of the counter. This arrangement results in a good definition of the geometry, in the sense that the angle by which a particle must scatter in the absorber to miss the final counter is not much different for any particle in the beam. It is also of great importance that the final counter have high efficiency when small attenuations are to be measured. We have used with good results a cylindrical vessel $2\frac{3}{4}$ inches thick, with a diameter of either $9\frac{1}{2}$ or 14 inches, filled with a xylene and terphenyl mixture. The sensitive volume is viewed by four RCA 6342 photomultipliers, immersed in the liquid. With a mixer circuit using four 6AK5's and no differentiating cable ("shorting stub") in the circuit, the $9\frac{1}{2}$-in. counter proved to be more than 99% efficient.

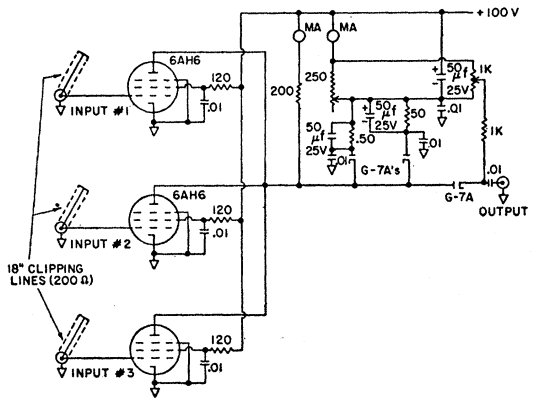

FIG. 5. Fast triple-coincidence circuit using grid clipping lines and a Garwin-type diode.

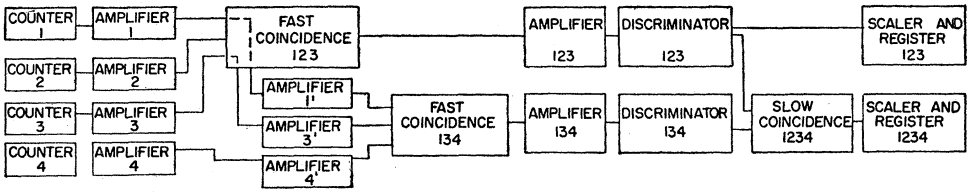

FIG. 6. Typical block diagram of the electronics used in the 40° direct beam and negative pion deflected beams using the circuit of Fig. 4.

C. Electronics

The repetition rate of the acceleration cycle of the Cosmotron is relatively slow (12–20 pulses per minute), and the time length of the burst which contains the particles of interest is short. By a suitable adjustment of the rate at which the rf accelerating voltage is turned off, this burst length can be varied from about two to twenty milliseconds. The counting rate of the circuits during a pulse is thus 100–1000 times greater than the total number of counts registered in one pulse. The counting rate for particles which cross the telescope has sometimes been as high as 10^5 sec^{-1}, and the counting rate in a single counter has been as high as a few times 10^6 sec^{-1}. For this reason coincidence circuits and their associated amplifiers and discriminators must have short resolving times and a minimum of dead time while maintaining a high efficiency.

Moreover, magnetically analyzed positive pion beams include protons of the same momentum. The ratio of protons to pions, which, of course, varies with the momentum and geometrical arrangement of the apparatus, is usually greater than one and has been as high as twenty-five. Since pions and protons of the same momentum differ in velocity, we can make use of the resulting difference in flight time through the defining telescope to separate the protons from the pions; that is, the resolving time and length of the telescope are so adjusted, for a given momentum, that the coincidence circuit records only the pions of the beam.

During the early phases of the work with negative pions, and positive pions below 1 Bev, coincidence circuits of the type shown in Figs. 4 and 5 were employed; a typical arrangement is shown in the block diagram of Fig. 6. The distributed constant amplifiers which precede the fast coincidence circuits have a rise time of 3 mμsec. The resolving time of the fast coincidence circuits, defined as the half-width at half-maximum, is approximately 4 mμsec. The amplifiers which follow the fast coincidence have a rise time of 0.03 μsec, the associated slow discriminators have a dead time of roughly 0.2 μsec. The fast scalers have a dead time of about 0.1 μsec.

In order to extend the range of positive pion measurements above 1 Bev using the 5.5° focused direct beam (Fig. 3), a more elaborate electronics arrangement was required. As the pion energy is increased, the time difference between the time of flight of a pion and a proton rapidly decreases. For example, with a counter separation of 35 ft as shown in Fig. 3, it decreases from 10.7 mμsec at 1 Bev to 3.8 mμsec at 1.80 Bev. At the same time, the ratio of protons to pions increases from about 5 to 25. Although the time difference could be increased by lengthening the telescope, two factors strongly favor keeping this length as short as possible. The first is the increase in muon contamination and the second is the decrease in total intensity which would result from lengthening the telescope. One wishes, therefore, to use the minimum length consistent with a clean separation of protons and pions.

The minimum difference of flight time necessary to distinguish pions from protons depends upon the time Δt in which the resolution curve of the coincidence circuit falls from an efficiency near unity to a sufficiently small value. In our beam, where the ratio of protons to positive pions R is about 10, the factor of decrease in efficiency, which we call the rejection ratio ϵ, must be $\sim 10^3$ in order that the fraction of protons recorded, R/ϵ, be $\sim 10^{-2}$. The resolution curve of a single pair of counters in a circuit of the type shown in Fig. 4 or 5 has a rejection ratio of only ~ 10 in a time $\Delta t = 4$ mμsec. In order to obtain the larger rejection ratio which we require in the same time, $\Delta t = 4$ mμsec, we make use of the following fact. The time required for a particle to cross a pair of counters is well defined by the momentum selection. We put into the beam (Fig. 3) three pairs of counters with each pair individually connected in coincidence using the circuit of Fig. 5. The outputs of the

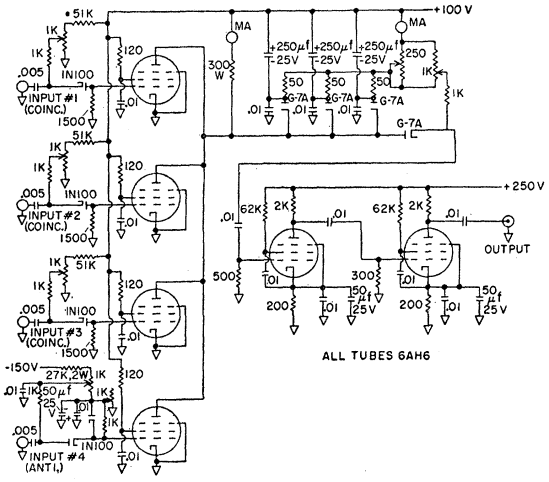

FIG. 7. Triple coincidence—anticoincidence circuit.

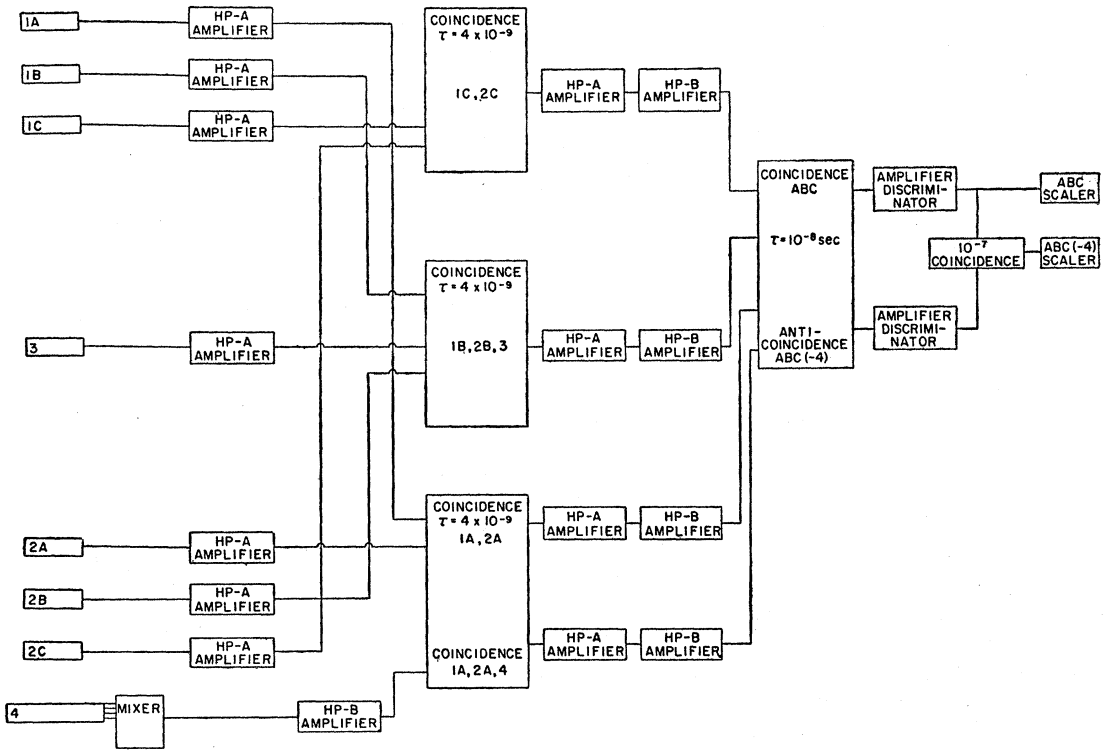

FIG. 8. Typical block diagram of the electronics for the 5.5° direct beam using the circuits of Figs. 5 and 7.

three separate pair coincidence circuits are then again placed in coincidence using the circuit of Fig. 7. Since each of the pairs of counters is independent, the rejection ratio of the combined system is the product of the rejection ratios of the separate pairs. We thus obtain a combined ratio of $\sim 10^3$ in $\Delta t = 4$ mμsec. A block diagram of the circuit arrangement is shown in Fig. 8. Typical resolution curves of the system, made by simultaneously delaying one counter of each pair, are illustrated in Fig. 9 for a beam momentum of 1.80 Bev/c. One curve is for a beam of pure pions, made by magnetically selecting negative pions; the other for a pure proton beam. The pure proton beam is obtained by lowering the energy of the primary protons which strike the target to 1.80 Bev. At this energy, the production of pions of momentum 1.80 Bev/c is not energetically possible; however, protons of this momentum are still present in the beam. If we arrange the cables to count pions at the point on the abscissa marked zero, the measured rejection ratio for protons is $0.34/1.5\times 10^{-4} = 2.3\times 10^3$.

For all our measurements, the recorded protons represent less than 1% of the pions. The magnitude of the correction for this contamination effect is too small to be important and it has therefore been neglected.

Since, in the 5.5° focused beam, the total intensity of pions plus protons is roughly 3×10^5 sec^{-1}, the circuits have been designed to minimize dead time; this is especially important in the channel which receives the pulses from the final counter. At these counting rates appreciable dead time would make the efficiency of the final counter rate dependent. Beam intensity fluctuations can then introduce a spurious effect. We have, therefore, avoided differentiation of the pulses in this channel. Tests at different beam intensities have shown that this effect with our arrangement is negligible.

D. Muon Contamination

Measurements of the muon contamination have been made for some of the beams used during the experiment. The origin of the muon is, for the most part at least, the pion decay, and this process is sufficiently well known that it is not necessary to repeat the measurement for each energy and position of the counter telescope. For one of the beams, we have also made detailed numerical computations using the UNIVAC computing machine of New York University. As examples of the measurements of the muon contamination, we describe the procedure followed for 0.55-Bev negative pions, 40° direct beam (Fig. 1) and for 1.5-Bev negative pions, deflected beam (Fig. 2).

We consider first the measurement at 0.55 Bev in the 40° direct beam. For purposes of discussion, it is convenient to divide the muons into two categories, (1) those which arise from pions decaying between the target and magnet $M2$, and (2) those which decay between $M2$ and the absorber. Muons in class (1) are subject to the same magnetic selection as the pions and have, therefore, the same momentum distribution as the

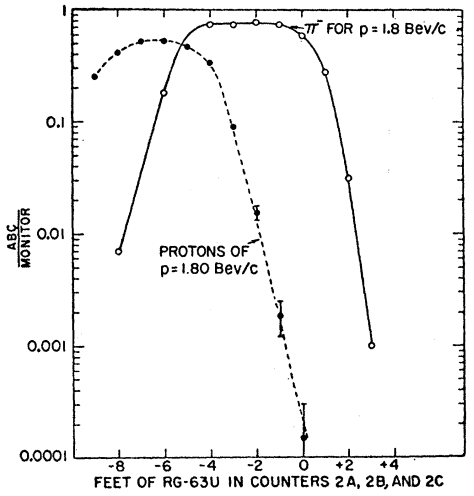

FIG. 9. Coincidence resolution curve for 1.80-Bev pions and protons in the 5.5° direct beam using the circuits of Figs. 5 and 7 and arrangement of Fig. 8.

selected pions. For muons in class (2), the parent pions have only a small momentum spread ($\pm 4\%$) around the selected momentum p_0, but the muons which result from their decay are spread uniformly in momentum between $0.57p_0$ and p_0. An experimental measure of the muons in category (1) and a fraction of those in category (2) can be made as follows.

The pions are strongly absorbed by nuclei, whereas muons are not. Therefore, if in the telescope which detects particles of one given momentum, an absorber almost as thick as the muon range is inserted, most of the pions, but none of the muons, will be removed from the beam by virtue of the strong pion-nucleon interaction. The ionization range of the muons is also larger than the range of the pions, but this is not of great help, because the telescope selects particles having a momentum spread of $\pm 4\%$. The corresponding spread of ranges for each of the two particles then leads to a large overlap. The momentum spread is necessary to attain reasonable intensities. Therefore, one must be careful to choose the maximum absorber thickness that does not stop the muons. We determined an absorption-range curve in iron for the pion-muon mixture, and plotted the coefficient of absorption $-dN/NdR$ (N = coincidence rate; R = absorber thickness). The curve in Fig. 10 shows an almost constant coefficient of absorption, due to the pion interaction, but at the absorber thickness equal to the minimum ionization range of the pions, the absorption coefficient shows a sharp rise. Once this point R_π is determined (Fig. 10), we can confidently decide at which thickness R_μ the muons will begin to be stopped by ionization. For this, we read from the known momentum-range curves the *difference* between the range of the pions and the range of the muons. If the absorption curve had been obtained with higher accuracy, it could actually have been "unfolded" and a more precise measurement of the muon contamination derived from it. For the present measurement, we take the rate of R_μ as an upper limit. The result for the curve of Fig. 10 is that the muons represent 6.5% of the beam. This measured number also contains a fraction of the muons which originated after the magnet (category 2). By using the known (rectangular) decay spectrum of the muon from pion-decay, this fraction can be computed. The total number of muons in category 2 (which originate after the magnet and cross our last counter) is then approximately computed, and the fraction of them which had already been counted is subtracted. The sum of the two categories gives the muon contamination, which is 12%. Because the computation tends to give too high a value, the assumed fraction is $10\pm 5\%$. That the break in Fig. 10 occurs at the correct range, within the estimated experimental error, can be checked from the momentum of the beam and from the available range-momentum curves. The momentum of the particles detected by the telescope was determined by the floating-wire method and by a range curve for the protons at the same magnet setting.

When the pion energy is high, for example, 1.5 Bev, the pion range is sufficiently large that almost all of them can be filtered out in an absorber before they reach the end of their range. That is to say, those particles which emerge from a suitably chosen absorber are, for the most part, only muons. The geometrical arrangement of absorber and final counter must be chosen in such a way as to minimize the number of muons scattered out of the final counter by multiple Coulomb scattering, so that the correction for this loss is not large. For the absorption curve of Fig. 11, taken with particles of momentum 1.63 Bev/c, the range of the least energetic muons from the decay of pions of that momentum is greater than 25 inches of iron. So, after 25 inches, all muons originally in the beam are still counted. The rate at 25 inches is 5.9% of the beam with no absorber. A correction for multiple Coulomb scattering raises this residue to 7.2%. A rough estimate of the

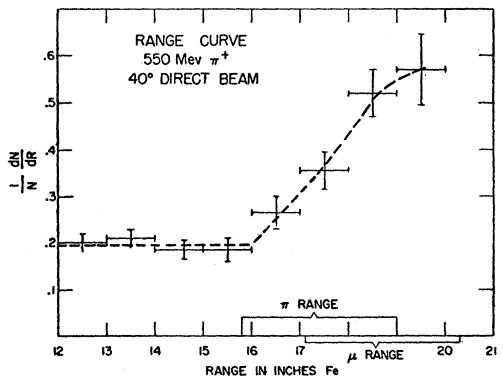

FIG. 10. The absorption coefficient $-dN/NdR$ as a function of range in iron for positive pions of kinetic energy 0.55 Bev (40° direct beam).

residual pions can be made, though it has little importance (2%). The muon contamination is then fixed at $5\pm3\%$.

For the 32° beam, we have made a numerical computation of the relative number of muons counted by the telescope. The digital UNIVAC computer of New York University was used, under the guidance of Dr. E. Courant who, together with H. Goertzel, coded the problem. The mean life and decay scheme of the pion are well known, as are the geometrical configuration of target, collimators, counters, and magnet. The pion production spectrum can be measured and, as the results show, need not be accurately known. Although the angular distribution of production is at present not known, one need only assume that it is isotropic over angles which differ by less than ±0.04 radian, an assumption which appears entirely reasonable. The problem was computed by using a Monte Carlo technique. In brief, the computation proceeds as follows: to each pion leaving the target five random numbers are assigned; four to the coordinates and initial angles at the target, and one, Z, which determines the point of decay, suitably weighted for the pion mean life. Each pion leaving the target is then followed either until it reaches the last counter as a pion or muon, or until it fails to stay within the required geometrical limitations at one of the constrictions representing collimators and counters.

Since the over-all probability that a pion decays is much smaller than one, the digital computer has to follow the trajectories of many pions in order to find one muon. A method is thus desirable to accelerate the decay. This objective cannot be reached by decreasing the pion mean life in the computation, since this method would change the distribution of decays along the path of the pions. The purpose is, however, achieved by taking, at the beginning, a random number as the value of the expression $Z=\exp(-x/vt)$, where x is the path length of the pion before decay, t the pion mean life in the laboratory system, and v the pion velocity. If Z is then required to fall within a smaller interval than from zero to one, the pion is "forced" to decay in a corresponding interval of x, without altering the natural distribution of decay points. For a given selection of magnet current (i.e., pion beam mean momentum), the initial energy of the pions leaving the target is varied stepwise to cover the entire range in which it is possible for a pion or muon to be accepted by the apparatus. In this way, we obtain curves of the probability of accepting a pion or a muon as a function of the initial energy of the pion. The muons are separated into two classes; those which arise from decays in front of the magnet, and those which decay after. The results of the Monte Carlo method are subject to a purely statistical error which depends on the total number of muons "detected." These errors are probably greater than those introduced by the assumptions and approximations involved. The contaminations so computed lie in the range 6–8% of the pion beams.

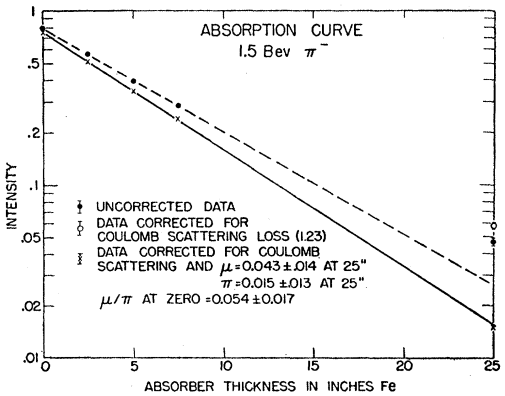

FIG. 11. The intensity of negative pions of kinetic energy 1.5 Bev as a function of range in iron (deflected beam).

For the 5.5° beam (Fig. 3) the muon contamination was computed approximately. The UNIVAC computation which had been made for three geometry-energy combinations served as a guide.

E. Electron Contamination

Electrons of the same momentum as the selected pions can constitute a contamination of the beam. The predominant origin of the electrons is the decay of neutral pions; they should thus be in equal numbers positive and negative and proportional to the intensity of the proton beam striking the target. Since the production ratio of positive to negative pions is greater than one, the percent of electrons in a negative beam is greater than that of positrons in a positive beam of the same energy. Hence, it is convenient to measure the contamination in the negative beams.

It was unnecessary to measure the electron contamination for all different beams that we used, especially since the measurements always showed that the contamination was of little importance. We thus made the measurement in the deflected beams of 1.0- and 1.5-Bev negative pions and in the 0.80-, 0.55-, and 0.45-Bev direct beams of positive and negative pions. It should be noticed that the 1.0- and 1.5-Bev beams are produced at 0° with respect to the primary protons, whereas the 0.80-, 0.55-, and 0.45-Bev beams are produced at 40°. The latter beams are thus expected to be contaminated most by electrons as well as muons.

The measurement was made in the following fashion: a lead radiator was inserted in the beam, and behind it two counters were placed, approximately side by side, to detect the electron showers produced in the lead. The efficiency of this shower detector can be approximately computed from the energy of the electrons and the thickness of the lead plate. For example, 0.94-Bev electrons, which are present in the beam of 0.80-Bev pions, produce in the radiator, on the average, eight electrons of energy larger than 8 Mev. Taking into ac-

TABLE I. Electron contaminations per unit negative pion beam as measured with an electron shower technique (Sec. IIE). Column 3 indicates the coincidence rate with lead radiator minus the rate with no radiator. Column 4, $\bar{N}$, is the average number of electrons at shower maximum having an energy greater than 7.8 Mev. Column 5 is the calculated efficiency of the shower detector. The measurements indicated by an asterisk in Column 1 were obtained by the method described in Sec. IIE.

Pion kinetic energy (Bev)	Electron kinetic energy (Bev)	Coincidence rate per unit beam	$\bar{N}$	Efficiency	Electrons per unit beam
1.50	1.63	0.0008±0.0003	12	0.23	≤0.0035±0.0013
1.00	1.13	0.0010±0.0005	8	0.15	≤0.007 ±0.004
0.80	0.93	0.0015±0.0022	8	0.27	≤0.0055±0.008
0.55	0.68	0.0027±0.0010	7.5	0.24	≤0.011 ±0.004
*0.45π^-	0.57				0.034 ±0.012
*0.45π^+	0.57				0.020 ±0.007

count the angular distribution, this leads to an efficiency of 27% for the shower detector. The computation of the efficiency is certainly not accurate, but the electron contamination turned out to be less than 1%, so that a more accurate determination was not needed. Table I gives the results of all the measurements.

At 0.45 Bev, the lowest energy for which we have cross-section measurements, the efficiency of the shower detector becomes rather low. For this reason, we have adopted a different technique. As we have already remarked, a direct beam such as the 40° beam must contain both positive and negative electrons in equal number. On the other hand, at 0.45 Bev the number of positive pions is 1.70 times the number of negative pions. The muons can be taken as proportional to the pions to an approximation good enough for the present purpose. If we then measure the ratio r of the number of positive to negative particles in the beam, including electrons and muons (not protons) and if, at the same time, we measure the ratio ρ of positive to negative pions, we can compute the relative number of electrons in the beam. ρ can be obtained by measuring the ratio of the rate of absorption of the positive beam (excluding protons) to that of the negative in a thin layer of carbon. In 40 g cm^{-2} carbon, only pions will be absorbed, while the electrons and muons are not much attenuated. Furthermore, charge symmetry requires that the absorption cross section in carbon for positive and negative pions be equal. The Coulomb field and inhomogeneity in the neutron-proton distribution cannot make important differences. The electron contamination α can then be obtained from ρ and r as follows. We have

$$\rho \equiv \pi^+/\pi^- = (\pi^+ + \mu^+)/(\pi^- + \mu^-),$$
$$r \equiv (\pi^+ + \mu^+ + e^+)/(\pi^- + \mu^- + e^-).$$

We define

$$\alpha^+ \equiv e^+/(\pi^+ + \mu^+), \quad \alpha^- \equiv e^-/(\pi^- + \mu^-).$$

Since $e^+ = e^-$, it follows that

$$r = (\rho + \alpha^-)/(1 + \alpha^-),$$

and

$$\alpha^- = (\rho - r)/(r - 1), \quad \alpha^+ = (1/\rho)[(\rho - r)/(r - 1)].$$

The result at 0.45 Bev is

$$\alpha^+ = 0.020 \pm 0.007, \quad \alpha^- = 0.034 \pm 0.012.$$

F. Coulomb Scattering in Hydrogen

The probability for the pions to be scattered out of the last counter by the hydrogen absorber is small for the measurements made with liquid hydrogen. Indeed, we derive[10] that one in a thousand mesons of 1.0-Bev/c momentum are scattered by more than 1° in the 2-g/cm^{-2} liquid hydrogen absorber. On the other hand, the rms angle for multiple scattering in the hydrogen is, for the same momentum, 0.17°. Our measurements were taken with a geometry (see Sec. IIA and IIB, also Fig. 3) such as to be unaffected by a scattering less than 3°. Hence we have applied no correction for Coulomb scattering in the cross sections determined with liquid hydrogen.

The measurements taken by C − CH_2 difference were, however, more affected by the Coulomb scattering for two reasons: first, the amount of hydrogen in the absorber sometimes reached 12 g cm^{-2}, and second, the multiple scattering in the carbon caused the beam to be less well defined at the last counter. In order to evaluate empirically an approximate Coulomb scattering correction, we insert small thicknesses of Pb scatterer interspersed with the C absorber, which is located in the same position as for the attenuation measurement. The Coulomb scattering effect introduced by the Pb should be very nearly the same as that of an equivalent number of radiation lengths of hydrogen.[11] Besides the Coulomb scattering effect, the Pb will introduce an attenuation due to nuclear interaction. For these small Pb thicknesses, the nuclear attenuation is considerably smaller than the attenuation due to Coulomb scattering and a corresponding correction can be applied. From the curve

TABLE II. Corrections to the cross sections for multiple Coulomb scattering in hydrogen which have been applied to the CH_2−C difference measurements. For the liquid hydrogen measurements, the correction for this effect is negligible.

Pion kinetic energy T_π in Bev (lab)	g cm^{-2} hydrogen	Anticoincidence angle θ_{rms} in degrees	Coulomb scattering correction in mb
0.45	3.9	6.3	−1.3
0.55	3.9	6.3	−0.3
0.55	3.9	3.2	−2.4
0.675	3.9	3.2	−1.7
0.79	3.9	3.2	−1.2
1.00	3.9	2.5	−0.3
1.00	12.17	3.2	−1.0
1.00	12.17	2.2	−2.0
1.50	8.27	2.5	−2.0
1.50	12.16	1.8	−2.9

[10] B. Rossi, *High-Energy Particles* (Prentice-Hall, Inc., New York, 1952), p. 65.

[11] It is, of course, to be expected that, for angles large compared to the rms angle of scattering, the distribution for Pb and H will differ due to the different size of the nuclei. See S. Olbert, Phys. Rev. **87**, 319 (1952). An approximate calculation for the difference indicates that it is always less than 0.7 mb. The hydrogen scatters more.

TABLE III. Summary of the total cross-section data.

Reaction	Kinetic energy T_π Bev (lab)	Kinetic energy T_π Bev (c.m.)	Available energy $T_\pi+T_p+\mu c^2$ Bev (c.m.)	$2\pi\lambda^2$ mb (c.m.)	Energy resolution $\pm\Delta T_\pi/T_\pi$ $\times 10^2$	Anticoincidence angle $\theta_{\rm rms}$ degrees	Muon contamination percent	Total cross section σ mb	Error (std. deviation) $\pm\Delta\sigma$ mb
$\sigma(\pi^-,p)$	0.45	0.264	0.48	17.0	4.3	6.3	10±4	28.8	2.7
	0.50	0.287	0.51	15.0	4.2	6.3	10±4	31.3	4.8
	0.55	0.309	0.54	13.4	4.2	3.2	9±4	37.4	3.0
	0.61	0.336	0.58	11.8	10.0	4.0	8.2±3	37.0	2.1
	0.67	0.362	0.62	10.5	4.1	3.2	8.5±4	39.5	3.0
	0.79	0.408	0.69	8.70	4.0	3.2	8.0±4	46.1	3.4
	0.86	0.435	0.73	7.87	5.0	4.0	7.5±3	47.7	2.7
	0.90	0.449	0.75	7.47	3.0	3.9	8.0±3	44.4	2.3
	0.97	0.474	0.78	6.83	5.0	4.0	7.5±3	45.1	2.7
	1.00	0.484	0.80	6.60	2.0	3.0	11.7±1.2	46.0	3.0
	1.08	0.510	0.85	6.03	5.0	4.0	7.5±3	36.3	2.6
	1.25	0.566	0.93	5.10	2.0	3.0	5.0±4	29.2	3.7
	1.35	0.597	0.98	4.67	5.0	4.0	7.5±3	30.1	2.8
	1.38	0.605	0.99	4.55	2.0	3.0	10.5±3	30.8	2.8
	1.47	0.632	1.04	4.25	3.0	3.9	8.0±3	31.4	1.8
	1.50	0.641	1.05	4.14	2.0	3.0	5.0±3	30.0	2.0
	1.67	0.687	1.13	3.66	2.0	3.0	9.5±3	31.4	3.9
	1.90	0.748	1.24	3.17	2.0	3.0	6.0±3	31.3	1.6
$\sigma(\pi^+,p)$	0.45	0.264	0.48	17.0	4.3	6.3	10±4	24.8	2.4
	0.55	0.309	0.54	13.4	4.2	3.2	9±4	16.1	2.5
	0.67	0.362	0.62	10.5	4.1	3.2	8.5±4	14.5	2.0
	0.79	0.408	0.69	8.70	4.0	3.2	8.0±4	19.5	2.0
	1.00	0.484	0.80	6.60	2.0	3.0	12±3	23.5	1.4
	1.07	0.495	0.84	6.10	2.0	3.0	10±3	27.3	3.7
	1.15	0.534	0.88	5.62	2.0	3.0	11±3	31.3	1.7
	1.25	0.566	0.93	5.10	2.0	3.0	10.5±3	38.8	2.5
	1.38	0.605	0.99	4.55	2.0	3.0	10.5±3	41.4	3.0
	1.50	0.641	1.05	4.14	2.0	3.0	10±3	35.3	2.5
	1.67	0.687	1.13	3.66	2.0	3.0	9.5±3	32.6	1.8
	1.77	0.715	1.18	3.44	2.0	3.0	9.0±3	31.7	2.4
$\sigma(\pi^-, d-p)$	0.79				4.0	3.2	8.0±4	16.1	3.0
	1.00				2.0	2.7	11.7±1.2	21.2	3.0
	1.25				2.0	3.0	5±4	33.3	4.0
	1.38				2.0	3.0	5±3	29.5	3.0
	1.50				2.0	3.0	5±3	27.0	4.0
	1.90				2.0	3.0	6±3	24.3	2.5
$\sigma(\pi^+, d-p)$	0.55				4.2	3.2	9±4	32.5	5.9
	0.79				4.0	3.2	8±4	41.4	3.5

of attenuation due to Coulomb scattering against thickness in radiation lengths, the effect of the number of radiation lengths of H introduced can be obtained directly. Such curves have been made for several pertinent energies and geometries. The resulting corrections are shown in Table II. Clearly, no such correction need be made to the measurements of the D_2O-H_2O difference.

III. RESULTS AND DISCUSSION

Table III summarizes our results for the cross section at each energy. Table IV is a compilation of the results of other authors in this energy range. At three energies [1.25 Bev, 1.38 Bev, and 1.67 Bev] a deviation in the (π^-,p) cross section appreciably more than the rms statistical error is present among the separate runs. While it is still possible that these deviations are due just to statistical fluctuations, considering the large number of individual measurements; nevertheless, for these cases the error we quote in Table III is the standard deviation computed from the deviations of the individual measurements. Figure 12 is a graphical plot of our data. Figure 13 shows the curves $\sigma(\pi^+,p)$ and $\sigma(\pi^-,p)$ as deduced from all of the available data. Assuming conservation of isotopic spin, the independent charge states of the pion-proton system are the two states having a total isotopic spin $T=\frac{1}{2}$ and $T=\frac{3}{2}$. The state $(T=\frac{3}{2})$ coincides with the state (π^+,p) so that $\sigma_{\frac{3}{2}}=\sigma(\pi^+,p)$. The cross section in the state $(T=\frac{1}{2})$ is

TABLE IV. Values of the total cross section above 0.45 Bev obtained by other authors.

Mean pion energy Bev	Total π^+ cross section in mb	Total π^- cross section in mb	Author[a]
0.45	27.5±6	25±3	LY
0.47		27±5	SLC
0.51		20±7	LY
0.60		23±11	LY
0.70	17 ±3	42±10	LY
0.84		47±5	SLC
4.4		30±5	BBMWW

[a] LY—S. Lindenbaum and L. Yuan[9]; SLC—Shapiro, Leavitt, and Chen[3]; BBMWW—Bandtel *et al.*[15]

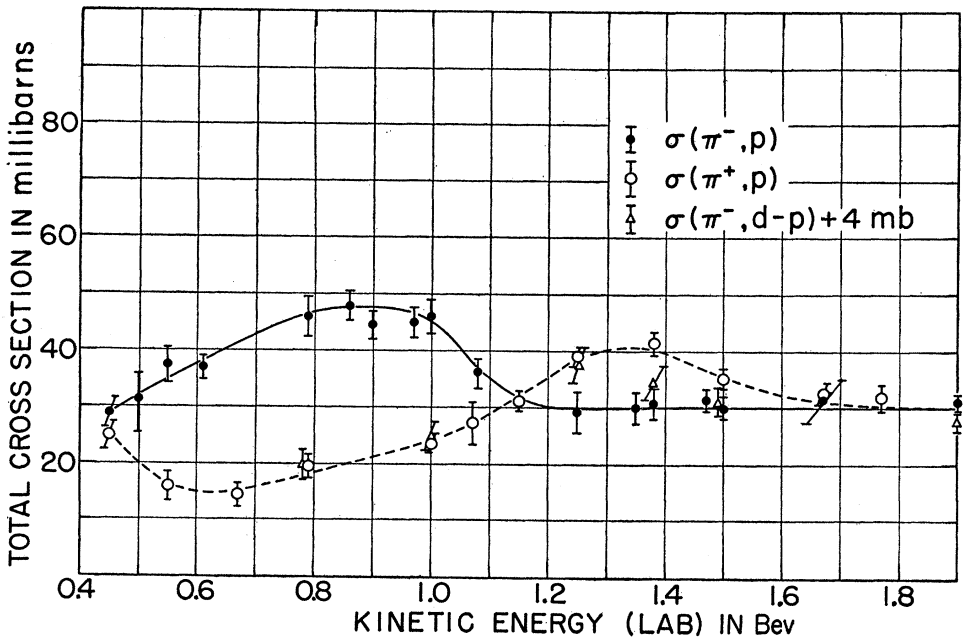

FIG. 12. Our results for the cross sections $\sigma(\pi^-,p)$, $\sigma(\pi^+,p)$, and $\sigma(\pi^-,d-p)+4$ mb. The addition of 4 mb to $\sigma(\pi^-,d-p)$ is a correction for the "shadow effect" in the deuteron. (See discussion at the end of Sec. III.)

given[2] by $\sigma_{\frac{1}{2}}=\frac{1}{2}[3\sigma(\pi^-,p)-\sigma(\pi^+,p)]$. The curve of $\sigma_{\frac{1}{2}}$ as a function of laboratory energy is also plotted in Fig. 13.

The minimum in the curve $\sigma_{\frac{1}{2}}$ at 1.38 Bev is, of course, a consequence of having drawn the curve $\sigma(\pi^-,p)$ as a line of constant cross section above 1.2 Bev. A curve $\sigma(\pi^-,p)$ having a small maximum at 1.38 Bev could also have been drawn through the experimental points, within their error, is such a way that $\sigma_{\frac{1}{2}}$ curve would indicate a substantially constant cross section for this state above 1.2 Bev.

Figure 14 shows the same curves plotted as a function of the total available energy ($\mu_\pi c^2$ included) in the center-of-mass system of the pion and proton. The curves of Fig. 14 can be used to derive other interesting quantities.

Recent theories which apply the causality principle to the scattering of particles with finite mass[12] have resulted in dispersion relations which make it possible to compute the forward scattering amplitude if the total cross section is known at all energies. For practical purposes, it appears sufficient to know the total cross section at energies only somewhat larger than the value at which the forward scattering amplitude is to be computed. Figure 15 reproduces the values of the real part (D) and Fig. 16 the imaginary part (I) of the forward amplitude in the laboratory frame of reference. D was computed by Sternheimer,[13] using the current values for the total cross sections,[14] including the result obtained at the Berkeley Bevatron,[15] $\sigma(\pi^-,p)=30\pm5$ mb at 4.4 Bev. The imaginary part $I(0°)$ of the forward scattering amplitude can be readily obtained from the relation $I(0°)=\sigma/4\pi\lambda$, all three quantities σ, λ, and $I(0°)$ are, of course, to be computed or measured at the same energy. As expected, the forward amplitudes reflect the oscillatory behavior of the total cross-section curves.

The curves for the real and imaginary parts of the forward amplitude allow us to compute, in principle with exactness, the differential cross section in the

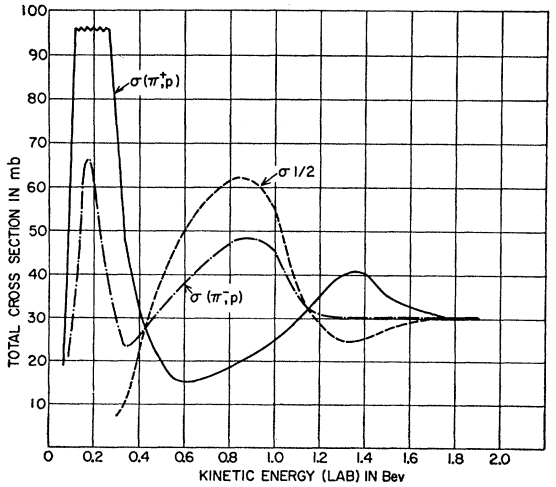

FIG. 13. The total cross sections $\sigma(\pi^+,p)$ and $\sigma(\pi^-,p)$ as a function of laboratory kinetic energy deduced from all experimental data. $\sigma_{\frac{1}{2}}$ is obtained on the assumption of charge independence.

[12] M. L. Goldberger, Phys. Rev. **99**, 979 (1955); Goldberger, Miyazawa, and Oehme, Phys. Rev. **99**, 986 (1955); R. Karplus and M. A. Ruderman, Phys. Rev. **98**, 771 (1955).

[13] R. M. Sternheimer, Phys. Rev. **101**, 384 (1956).

[14] We are grateful to Dr. R. M. Sternheimer for making these computations available to us. The curves published in reference 13 were based on our earlier data before π^+ measurements were made above 1.0 Bev. Compare Anderson, Davidson, and Kruse, Phys. Rev. **100**, 339 (1955).

[15] Bandtel, Bostick, Moyer, Wallace, and Wikner, Phys. Rev. **99**, 673 (1955).

forward direction for elastic scattering and for charge exchange for all combinations of charge signs of the nucleon and the pions. Figures 17, 18, and 19 show these differential cross sections. In the figures, the contribution of the real part of the respective amplitudes to the cross section is separately indicated; the contribution of the imaginary part can obviously be obtained by difference. One sees that the forward scattering is preponderently due to the imaginary part at energies above 0.8 Bev for $d\sigma^+(0°)/d\Omega$ and above 0.4 Bev for $d\sigma^-(0°)/d\Omega$. At 1.37 Bev we can compare the forward differential scattering $d\sigma^-(0°)/d\Omega$ given by the curve of Fig. 18 with the experimental value obtained by the Brookhaven Cloud Chamber Group.[16] A conversion to the center-of-mass system is most easily accomplished by noting that the quantity $\lambda^2 d\sigma/d\Omega$ is invariant. Curve 18 gives $d\sigma/d\Omega = 35$ mb/sterad in the laboratory system, therefore $d\sigma/d\Omega = 9$ mb/sterad in the c.m. system. The experimental value is 13 mb/sterad. The difference between these two numbers is no larger than the error.

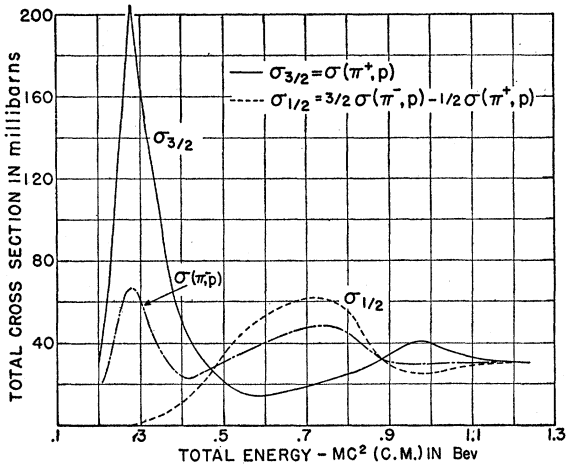

FIG. 14. The total cross sections $\sigma(\pi^+,p)$, $\sigma(\pi^-,p)$, and $\sigma_{\frac{1}{2}}$ as a function of the total energy available in the center-of-mass system (less the rest energy of the nucleon). $\sigma_{\frac{1}{2}}$ is obtained on the assumption of charge independence.

In the same way, the data of Walker[17] at 1.0 Bev, which gives $d\sigma^-(0°)/d\Omega = 14 \pm 2$ mb/sterad c.m., is to be compared to the computed value of 13 mb/sterad. A phase shift analysis of the recent data of Margulies[18] allows the real part of the forward amplitude D^+ to be obtained directly from the experiment. His values for D_{lab}^+ are $(-1.05 \pm 0.22) \times 10^{-13}$ cm at 0.258 Bev, $(-1.32 \pm 0.22) \times 10^{-13}$ cm at 0.294 Bev, and $(-1.41 \pm 0.37) \times 10^{-13}$ cm at 0.395 Bev. These values are all in excellent agreement with the computed values of Fig. 15.

The charge exchange scattering of Fig. 19 is of particular interest. For this type of scattering, the real part plays an important role up to high kinetic energies. An experimental check on the amount of the "elastic" charge exchange scattering at 1.0 and at 1.4 Bev would constitute an important check on the dispersion relations and on the validity of the charge independence principle at this energy. It is indeed quite obvious that if the (π^+,p) system were independent of the (π^-,p) system, contrary to the implication of charge independence, then our prediction for the amount of charge exchange scattering would be entirely groundless. It should be noticed that, unfortunately, the predicted differential cross section for charge exchange is quite small, probably smaller than the differential cross section for the production of neutral pions in the inelastic collisions. An experimental check would, therefore, require some determination of the spectrum of the secondary gamma rays.

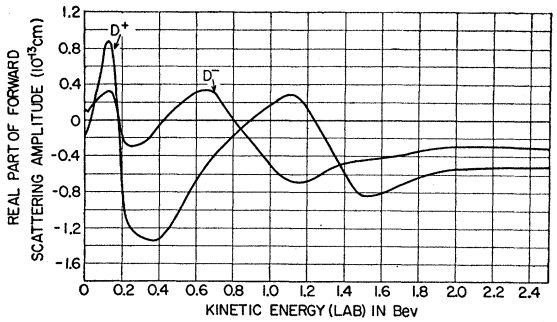

FIG. 15. The real part of the forward amplitude for elastic scattering of positive and negative pions as a function of laboratory kinetic energy.

Returning to the curves of Figs. 13 and 14, one sees that, in addition to the well-known first maximum at 190 Mev for $\sigma_{\frac{3}{2}}$, a second maximum is unquestionably shown. The maximum occurs for $\sigma_{\frac{3}{2}}$ at an energy in the vicinity of 0.9 Bev. The curve is asymmetrical with respect to the 0.9-Bev abscissa in the plot of σ *versus* kinetic energy in the laboratory system; this behavior is quite different from that of the first maximum. At an

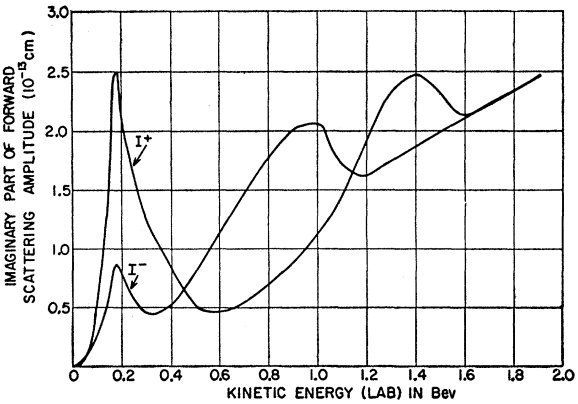

FIG. 16. The imaginary part of the forward amplitude for elastic scattering of positive and negative pions as a function of laboratory kinetic energy.

[16] Eisberg, Fowler, Lea, Shephard, Shutt, Thorndike, and Whittemore, Phys. Rev. **97**, 797 (1955).
[17] W. D. Walker (private communication).
[18] R. Margulies (private communication).

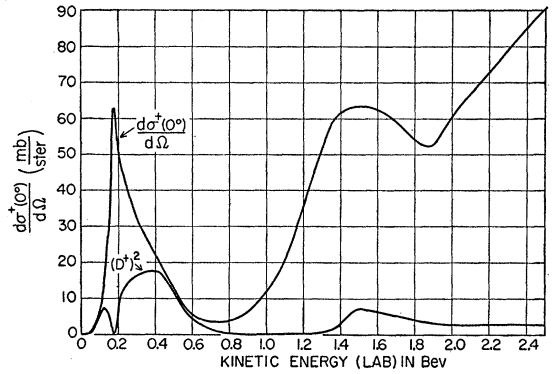

FIG. 17. The differential cross section for elastic scattering at zero degrees of positive pions ($\pi^+ + p \rightarrow \pi^+ + p$) as a function of laboratory kinetic energy. The curve marked $(D^+)^2$ is the contribution to the differential cross section from the real part of the forward amplitude alone.

even larger energy, namely at 1.38 Bev, a third maximum seems to occur for $\sigma_{\frac{3}{2}}$, and this time the curve again shows a good measure of symmetry. Since the communication of our preliminary results, some attempts have been reported by Mitra,[19] Dyson,[20] Takeda,[21] and Feld[22] to fit the curves of Fig. 13, and especially the second maximum, into the current ideas about the interaction between pions and nucleons. The problem still remains substantially unsolved. The curves themselves do not furnish such convenient clues for the explanation of the second maximum, as they do for the maximum in $\sigma_{\frac{3}{2}}$ at 190 Mev. There, as we have already mentioned, the cross section reaches almost exactly the value expected for a resonance in a state of total angular momentum $j=\frac{3}{2}$. Such a fortunate situation does not exist at 0.9 Bev, and, of course, it is *a priori* improbable at that energy to have an extreme preponderance of the interaction in one single state of angular momentum.

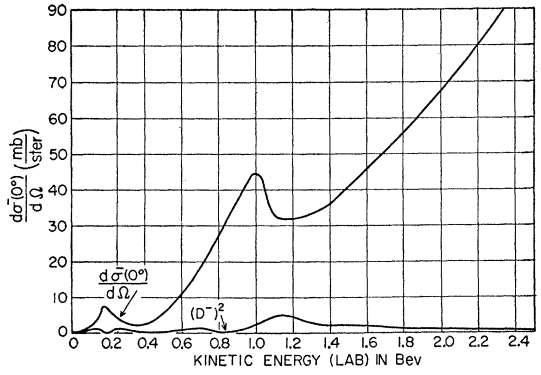

FIG. 18. The differential cross section for elastic scattering of negative pions at zero degrees ($\pi^- + p \rightarrow \pi^- + p$) as a function of laboratory kinetic energy. The curve marked $(D^-)^2$ is the contribution to this process from the real part of the forward amplitude alone.

[19] A. N. Mitra, Phys. Rev. **99**, 957 (1955).
[20] F. J. Dyson, Phys. Rev. **99**, 1037 (1955).
[21] G. Takeda, Phys. Rev. **100**, 440 (1955).
[22] B. T. Feld, Bull. Am. Phys. Soc. Ser. II, **1**, 72 (1956).

One can only obtain a minimum value for j such that a resonance in that state alone, plus a nonresonant interaction in other states, could together add up to the experimental value. An appreciable amount of estimating is necessary even for this limited aim. First of all, at this energy one is inclined to assume the validity of the principle of the conservation of isotopic spin. Strong evidence for this principle exists at energies around 200 Mev, but none at 1 Bev. A consequence of the assumption that the principle is valid is that a maximum value of about 60 mb, instead of 40 mb, must be explained. This follows immediately from inspection of Figs. 13 and 14. Another rather arbitrary decision must be made in order to subtract the contribution of the nonresonant states from the total cross section near 0.9 Bev. One might take the contribution to be equal either to the value of $\sigma_{\frac{1}{2}}$ beyond the maximum at 1.2 Bev, or to $\sigma_{\frac{3}{2}}$ at 1 Bev. Lacking good theoretical criteria,

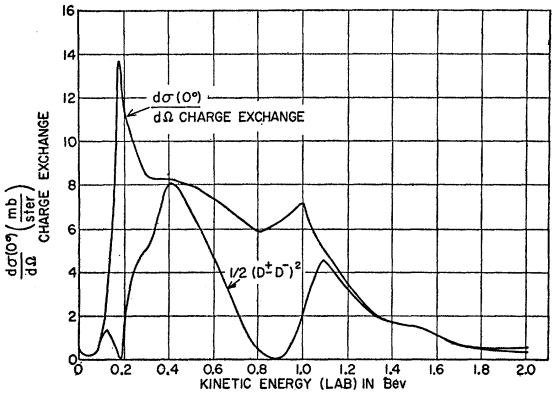

FIG. 19. The differential cross section for charge exchange scattering of negative pions at zero degrees ($\pi^- + p \rightarrow n + \pi^0$) as a function of laboratory kinetic energy. The curve marked $\frac{1}{2}(D^+ - D^-)^2$ is the contribution to this process from the real part of the forward amplitude alone.

we tend to favor the following argument. The curves seem to show oscillations superimposed on a nonresonant cross-section term which is very low at about 0.4 Bev and which reaches a constant value equal to 30 mb at energies higher than 1.2 Bev. Figure 20 shows the result of subtracting such a term (curve marked A in Fig. 20) from $\sigma_{\frac{3}{2}}$ and $\sigma_{\frac{1}{2}}$. The curve $\sigma_{\frac{1}{2}}$ then appears less asymmetric, and the second maximum is slightly displaced to a lower energy, about 0.77 Bev. On the basis of Fig. 20, we must attribute to the resonant state a cross section of about 42 mb. It would not make much difference if we had taken the value at an energy higher than 1.2 Bev.

Now, the maximum cross section $\sigma_M(j)$ for a state of orbital angular momentum l and total angular momentum $j=l\pm\frac{1}{2}$ can easily be determined, given the energy at which the maximum occurs, if the reaction responsible for the resonance is pure elastic scattering. For an inelastic reaction, the maximum cross section

cannot be *a priori* determined. Yang,[23] however, has pointed out an inequality which allows us to determine $\sigma_M(j)$ if the ratio between the cross section for elastic scattering σ_e and the total cross section σ_t is known for the same state of angular momentum j:

$$\sigma_M(j)=2\pi\lambda\!\!\!^{-2}(2j+1)\sigma_e/\sigma_t.$$

No determination of σ_e/σ_t is available at 0.77 Bev. The closest energy at which such a ratio has been measured is 1.0 Bev, in the hydrogen diffusion cloud chamber of the Brookhaven group. Walker[17] has analyzed the photographs and found $\sigma_e/\sigma_t\cong 0.5$. This value refers to *all* events occurring at 1.0 Bev, and not just to the one angular momentum state responsible for the second maximum.

If we use the ratio $\sigma_e/\sigma_t=0.5$, keeping in view that it has not been obtained at the correct energy and that it

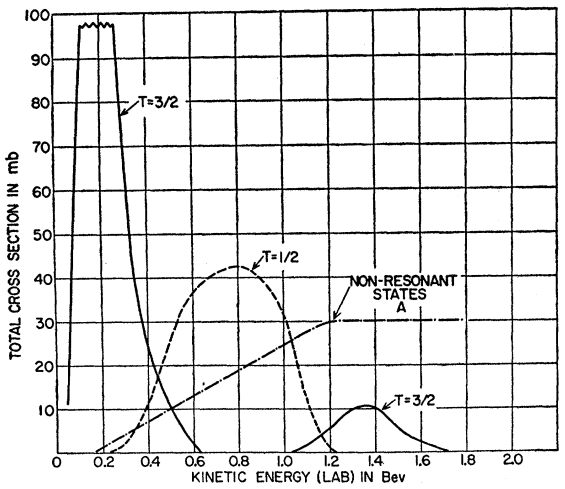

FIG. 20. The cross sections $\sigma_{\frac{3}{2}}$ and $\sigma_{\frac{1}{2}}$ as a function of laboratory kinetic energy after the subtraction of a contribution from nonresonant angular momentum states which has been assumed to take the form of the curve marked A.

is not for a single j value, one determines j from the relation: $42\text{ mb}\leq 2\pi\lambda\!\!\!^{-2}(2j+1)(0.5)$. Since $2\pi\lambda\!\!\!^{-2}=9$ mb at 0.8 Bev, one obtains $j\geq 8.3/2$. A change in the ratio σ_e/σ_t from 0.5 to 0.78 would, however, change this inequality into $j\geq 5/2$. Considering that the relative contribution of the various states at 1.0 Bev may not be the same as at 0.77 Bev, we conclude that the assignment $j=5/2$ is quite compatible with the experimental data. An attractive suggestion which would not require that a single state produce the second maximum has been advanced by Feld.[22] He considers the possibility that more than one angular momentum state passes through a maximum so that an overlapping of these resonances could account for the observed effect. All of the states would have $T=\frac{1}{2}$ but different j values (e.g., three states with $j=\frac{1}{2}$, $\frac{3}{2}$, $\frac{5}{2}$, respectively), each leading to a final state consisting of a nucleon isobar ($j=T=\frac{3}{2}$, total energy $Mc^2+\mu c^2+150$ Mev) plus a p-wave pion. In this way it seems possible to explain a curve having the asymmetrical shape indicated by the experiment, while the need for a high-j state would disappear entirely.

Another approach to the problem of the second maximum has been reported by Dyson[20] and Takeda.[21] We had, independently, also started to think along the same line, but had been discouraged by a difficulty which will be mentioned in what follows.

The approach consists in imagining that the interaction between a pion and a proton occurs mainly via an interaction of the bombarding pion, π_b, with a virtual pion, π_v, emitted by the proton. The idea stems from the analogy with the collision of high-energy protons with nuclei. In that case, we know that it is quite fruitful to think of the reaction as a collision between the bombarding proton and one of the nucleons contained in the nucleus. Clearly enough, the model loses its definition when extended to the pion-proton collision. Whether the model can be of any use depends entirely on the range, strength, and nature of the interactions involved. However, if one accepts the model, an advantageous point is that the maximum cross section for a state of angular momentum j in the center-of-mass system of π_b and π_v is much larger than for a state of angular momentum j in the center-of-mass system of the pion and the proton. In order to obtain an effect in the state $T=\frac{1}{2}$ for the pion-proton system, and no effect for $T=\frac{3}{2}$, Dyson chooses to assume that the pion-pion interaction occurs, at least preponderantly, in the $T=0$ state for the pion-pion system. Because the pion is a boson, only even values for l are then allowed. The maximum cross section for the pion-pion interaction in a state $T=0$ and even l is given by $(8\pi/3)\lambda\!\!\!^{-2}(2l+1)\sigma_e/\sigma_T$. The quantity σ_e/σ_T can be put equal to one, since most of the inelastic pion-proton collisions resulting in two secondary pions could be interpreted as π_v being knocked out of the nucleon structure. For a bombarding energy of 0.77 Bev in the center-of-mass system of the two pions (π_v considered at rest), the whole system has a total energy of about $4\mu c^2$, each meson has a kinetic energy of 0.130 Bev, a momentum of 0.23 Bev/c, and $\lambda\!\!\!^{-}=0.86\times 10^{-13}$ cm. The quantity $(8\pi/3)\lambda\!\!\!^{-2}(2l+1)$ equals 62 mb for $l=0$, and 310 mb for $l=2$. As already stated, the large values for the cross section which are possible for a pion-pion collision constitute the main attractive feature of the model. An unattractive side of it is that the virtual meson has a finite momentum of its own. If π_v has a momentum q, and a corresponding total energy ω, the impinging meson π_b with a momentum p ($pc\cong$total energy for a pion of energy $\sim$1 Bev) is seen by π_v as having any energy with equal probability in the interval with end points at $(\omega\pm qc)p/\mu c$. This interval is $2qp/\mu$ wide, and if $q/\mu c\sim 1$ and $pc\sim 1$ Bev, the spread measures $\sim$2 Bev. When the momentum p is varied, the aver-

[23] C. N. Yang, *Proceedings of the Fifth Annual Rochester Conference on High Energy Physics* (Interscience Press, Inc., New York, 1955), p. 37.

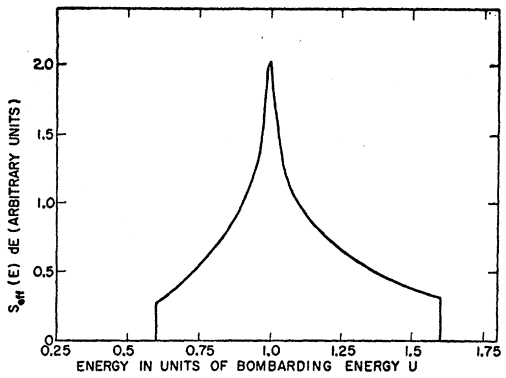

FIG. 21. The effective energy spectrum in a pion-pion collision for a bombarding pion of total energy U(lab) and a virtual pion spectrum which is constant from $k=0$ to $k=0.5\ \mu c$. The energy is plotted on the abscissa in units of the total energy U.

aging over such a large interval would have the effect of smoothing out any resonance that the pion-pion system might have. Therefore, the success of the model depends on the spectrum $S(q)$ that should be attributed to the virtual pions. For example, Fig. 21 shows the energy spectrum of the bombarding pions of total energy U as seen by the virtual pions, when $S(q)$ is equal to a constant from $q/\mu c=0$ to $q/\mu c=0.5$. For such a spectrum, it would be possible for the $\sigma(\pi^-,p)$ curve to show marked effects due to pion-pion resonances.

If the pion-pion interaction has an appreciable importance in pion-proton collisions, one could perhaps detect its effect in the distribution among the possible final states of an interaction when two or more mesons are produced. Consider the case $\pi^-+p\rightarrow p+\pi^0+\pi^-$. If the two-pion system has a resonance when the total energy W in *their* center-of-mass system equals a certain value W_r, then the states for which $W=W_r$ should be relatively preponderant. One can see that the vector momentum of the outgoing proton alone determines W if the bombarding pion momentum is known. This latter need not, in principle, have any particular value. We have, therefore, tried to see whether any evidence for the pion-pion model could be found in the cloud chamber results of Eisberg *et al.*[16] These authors plot the momentum distribution (c.m.) of the protons and of the neutrons, produced respectively in the reactions

$$\pi^-+p\rightarrow p+\pi^0+\pi^-,$$
$$\pi^-+p\rightarrow n+\pi^++\pi^-,$$

obtained with pions of kinetic energy $=1.37$ Bev. The neutron spectrum has a maximum at $p=0.55$ Bev/c while the proton spectrum probably does not. The neutron momentum at the maximum would give $W_r=0.6$ Bev, while interpreting our $\sigma(\pi^-,p)$ with the pion-pion model, we would obtain $W_r=0.56$ Bev. The possible absence of the maximum for the protons would agree with Dyson's choice that the pion-pion system interacts strongly for the above value of W_r and total isotopic spin $=0$. This little encouragement is reduced if one computes the expected distribution for the neutron momentum in these events on the simple basis of state density in phase space as a function of neutron momentum. The spectrum computed in this way also has a maximum at a momentum not much higher than observed experimentally.[24] Of course, the actual spectrum does not need to follow the phase space distribution, and the comparison with the momentum spectrum for the outgoing protons (in the reactions that produce π^0's) could be illuminating if the statistical uncertainty were reduced. Thus the available cloud-chamber data are not conclusive, but perhaps more systematic research on this line might be justified. The curves of Figs. 12, 13, 14, and 20 show the presence of a third maximum, which seems to be present for the $T=\frac{3}{2}$ wave only. The ratio of the amplitude of the oscillation to the statistical and systematic error is here less favorable than at the second maximum. However, if we take into account that, for the purpose of comparing adjacent points, the errors should be somewhat reduced, we must conclude that the third maximum very likely exists.

The shape of the curve at the third maximum is reminiscent of the first, except for the amplitude of the oscillation. The value of $\sigma(\pi^+,p)$ at the maximum is 41 mb which is small enough that even a $j=\frac{3}{2}$ wave could account for it, if we again subtract the contribution of the nonresonant states as in Fig. 20.

The data for $\sigma(\pi^-, d-p)$, obtained from the difference in the attenuation of water and heavy water, were taken for the purpose of measuring approximately the cross section $\sigma(\pi^+,p)$ at a time when a positive pion beam was not available at high energies (see discussion in Sec. IIA). In the last stage of this work, positive-pion beams were obtained, and therefore, we can now use the deuterium data to determine the magnitude of the "shadow effect," which is the term commonly applied to the fact that the total cross section of deuterons is less than the sum of the total cross sections of free neutrons and protons. The analogy with geometrical optics, which obviously suggests that name, is of course rather crude. In fact, if we compute the light intercepted by two spheres of radii r_1 and r_2, separated by a distance R, larger than r_1 and r_2, then we find $\sigma=\sigma_1+\sigma_2-\sigma_1\sigma_2/2\pi R^2$ where $\sigma_1=\pi r_1^2$; $\sigma_2=\pi r_2^2$.

Instead, Glauber,[25] using wave mechanics, finds that $\sigma=\sigma_1+\sigma_2-\sigma_1\sigma_2/4\pi R^2$ when the spheres have no refractive properties, which indicates a shadow effect one-half as large as that suggested by the classical computation. The difference can be seen to originate from the coherent diffraction scattering of the two spheres, and it is independent of the ratios $\sigma_{1\ \text{elastic}}/\sigma_{1\ \text{absorption}}$ and $\sigma_{2\ \text{elastic}}/\sigma_{2\ \text{absorption}}$ which are determined by the transparencies of the particles 1 and 2, if both are nonrefractive. Furthermore, as Glauber points out, if σ_1, σ_2,

[24] We thank Dr. C. J. Goebel for his kind help in connection with this computation.

[25] R. J. Glauber, Phys. Rev. **100**, 242 (1955).

and σ are absorption cross sections only, with neglect of elastic events, then the classical expression is correct. Including the refractive properties of the neutrons and proton, Glauber obtains $\sigma=\sigma_n+\sigma_p+4\pi\lambda^2\,\mathrm{Re}[f_n(\theta)f_p(\theta)]\langle r^{-2}\rangle_d$ in the limiting case when the two nucleons are at large distances apart. λ is the wavelength of the meson in the laboratory system, $f_n(\theta)$ and $f_p(\theta)$ are the forward scattering amplitudes, and σ_n and σ_p are the total cross sections of the neutron and proton for (π,n) and (π,p) collisions. r is the distance between the two nucleons, and the symbol $\langle\ \rangle_d$ indicates the operation of averaging according to the deuteron wave function. Glauber has checked that the above expression gives a $\delta\sigma=\sigma_d-\sigma_n-\sigma_p$ which differs by only 20% from a more exact relation that is valid at small separations. From the simple expression above, and from Figs. 15 and 16, we can see that for the energies of interest to us the forward amplitudes can be replaced by their imaginary parts. We can then use the computation of Glauber, who has computed the shadow effect, using three different choices for the wave function of the deuteron. We thus find that the wave function corresponding to a square well potential gives $\delta\sigma=4.2$ mb, the Hùlthen function gives 5.3 mb, and a potential which includes a hard core of radius $r_c=0.531\times10^{-13}$ cm gives 3.3 mb. All three values are substantially unchanged for energies above 0.8 Bev. Our best value for this effect is for 0.79 Bev, where all the necessary measurements were taken under the same conditions so that the error due to the contaminations is reduced. We obtained the difference $\sigma(\pi^-,p)-\sigma(\pi^+,d-p)$ which by charge symmetry is equal to $\delta\sigma$ for negative pions. Inverting the charge of the pions, we also obtained $\delta\sigma$ for positive pions. The result was $\delta\sigma(\pi^+)=3.4$ mb; $\delta\sigma(\pi^-)=4.7$ mb. Their average is 4 ± 2 mb. Moreover, the smallness of the difference, $\delta\sigma(\pi^-)-\delta\sigma(\pi^+)=1.3\pm3.5$ mb, constitutes a check on the principle of charge symmetry. The deuteron cross sections obtained by the addition $\sigma(\pi^\pm,p)+\sigma(\pi^\pm,d-p)$ turned out to be $\sigma(\pi^+,d)=60$ mb and $\sigma(\pi^-,d)=62$ mb for a pion kinetic energy equal to 0.79 Bev.

If we use all the independent measurements (see Table IV) from which we can derive a value for $\delta\sigma$, and we average them all irrespective of their energies, which are distributed between 0.79 and 1.5 Bev, we obtain $\delta\sigma=6\pm2$ mb. Substantially all three theoretical values can be considered in agreement with both of the experimental effects we have quoted.

ACKNOWLEDGMENTS

It is a pleasure to acknowledge the active collaboration of Professor L. Madansky during the early part of this work while he was on leave from The Johns Hopkins University; of Dr. J. Cronin and Mr. A. Abashian who joined us during the final stages of the measurements; of Mr. C. F. Woolley, Jr., who assisted us throughout the course of these experiments.

We are greatly indebted to Professor R. Serber, Dr. K. A. Brueckner, Dr. H. S. Snyder, and Dr. R. M. Sternheimer for valuable and illuminating discussions.

We wish to thank Dr. S. A. Goudsmit and Dr. G. B. Collins for their encouragement and support and the operating staff of the Cosmotron for their cooperation.